

## Chapter 3

# Structure and selection in an engineered symbiotic biofilm consortium

*Portions of this chapter are in submission [50].*

### 3.1 Abstract

Microbial consortia constitute a majority of the earth's biomass, yet the evolutionary mechanisms by which they arise are debated. How do communities survive despite fitness differences, and therefore competition, between their constituents? Theory suggests that a community may adopt a spatial configuration, an "emergent structure," which gives the community a growth advantage over its members; natural selection can preserve a community if this structure and its growth advantage can be transferred to downstream environments. We present a synthetic symbiotic consortium in which two otherwise nonviable populations of genetically engineered *Escherichia coli* can complement each other, grow, and form biofilms. By exploring growth of the symbiotic biofilm through time, we discover emergent structure that can be transferred to downstream environments. When aggregates of the two populations are preserved through population bottlenecks, the emergent structure and a growth advantage are transferred to downstream environments, but when the aggregates are disrupted neither the emergent structure nor the full growth advantage is transferred. From such engineered consortia we may decipher some of the mechanisms that underlie the persistence of consortia in nature.

## **3.2 Introduction**

The vast majority of living biomass consists of single-celled organisms, but the existence of higher organisms implies that natural selection can conserve interacting networks of cell populations despite competition between them [76, 77]. How nascent communities gain a growth advantage over their constituents is debated [47, 78-81], but highly complex cell–cell interactions [15, 29, 82-84], formation of multi-cellular structures [28, 85, 86], and the rise of genetic polymorphisms in spatially heterogeneous environments [87, 88] might contribute. Evaluating the role of emergent structure in evolution of natural communities poses a causality dilemma [77], yet *de novo* design of synthetic communities that exhibit emergent structure is difficult, so demonstrations of selection acting upon structure to preserve communities are few. It is known that competitors may coexist when cell–cell interactions occur over a small spatial scale between consistent neighbors through time, as they do in biofilm environments [89-92]. Additionally, emergent structure can arise when two populations that do not normally interact in nature are cultured together in a biofilm [93]. We set out to explore structure in a microbial community by engineering a synthetic symbiotic biofilm consortium.

## **3.3 Background: Evolution of communities**

### **3.3.1 Kin selection**

Theory suggests that multi-cellular entities can evolve from cooperating populations of single cells [94]. However, the mechanisms that provide for cooperating populations to survive in the face of cheats, individuals that take advantage of cooperation without assisting it, are not entirely clear. Therefore, to understand one path by which multi-

cellular organisms might have arisen, we must first understand the rise of cooperation in groups of individual cells. Kin-selection, or group-selection, theory proposes one mechanism by which cooperation can arise and become stable despite competition [95].

Kin- and group-selection were once considered separate entities but are now understood to be alternative statements of the same effect [96]. Kin-selection theory says that altruism, or gene expression that benefits a group at the expense of the individual, is more likely to arise in populations that exhibit less genetic diversity [85]. Thus, in a community where altruists are predominantly surrounded by other altruists, the outcome of a conflict between selection at the level of the individual (non-altruists are more fit, because they do not incur the cost of cooperation) and selection at the level of the group (individuals benefiting from cooperation are more fit) can be survival and dominance of the altruists. Stated another way, altruists must be the primary beneficiaries of the costly cooperative behavior in order for it to arise and become stable in a population. In one sense, then, kin-selection is selection at the level of the individual. However, the evolutionary outcome of the population cannot be predicted without knowledge of what is happening at a higher level of organization. That is, to predict the outcome we must examine not just fitness, but inclusive fitness, of the altruistic gene or genes [77]. Inclusive fitness takes into account the reproductive success of all individuals in a population possessing a given gene. The inclusive fitness of altruists depends upon how many of them are present, and/or upon how they are oriented in space with respect to one another.

### 3.3.2 Experimental demonstrations of community selection

Simple experimental demonstrations of how cooperation is maintained in laboratory populations exist. Many start with uniform populations of cooperators and observe the rise and impact of cheating subpopulations. For example, studies of *Pseudomonas fluorescens* reveal that cheats are more likely to take over through evolution when a population experiences large bottlenecks (many individuals from one community are propagated to the next) [97]. In contrast, when only a few individuals survive population bottlenecks, the survivors are more likely to be related and cooperation is thereby maintained. The same authors also show that cooperators can be selected when population bottlenecks occur at intermediate frequencies with respect to time (without regard to size), and that productivity in resulting populations is optimized [98, 99]. Importantly, spatial alignment between the bacteria was not preserved during bottlenecks in either study—cultures were homogenized during bottlenecks—so propagation was by truly random selection. As a result, the only factor determining survival of cooperation was the ratio of cooperators to cheats. In nature cells can stick together to form clusters, or aggregates, and these aggregates can be transferred between environments. It would be interesting to see how preserving aggregates through population bottlenecks might change the results of studies like these.

*Pseudomonas aeruginosa* is another common laboratory species that has been studied to examine the evolution of cooperation. For example, one challenge to kin selection arises under the condition where nutrients are limited. In this case, relatives living in close proximity become competitors (over a limited food supply) as well as cooperators, complicating the evolutionary outcome. One study examined this

phenomenon by varying both the relatedness of and the degree of competition in different cultures of *P. aeruginosa*. They showed that cooperation is advantageous in the face of global competition between subpopulations, despite the mitigating force of local competition within the subpopulations [100]. In another study, the authors watched the rise of quorum-sensing cheaters in populations of *P. aeruginosa*. The authors found that high relatedness allowed quorum-sensing variants to survive because cheaters were often localized in separate subpopulations. When populations began with lower relatedness, cheaters increased in frequency to a limit (the limit was determined by the fact that cheaters require the altruistic behavior of cooperators for optimal growth) [48]. In this latter set of experiments spatial structure was given no consideration, and in neither study did the authors examine whether the bacteria aggregated. Here again, it would be interesting to explore how spatial structure that arises and aligns the bacteria with one another impacts these studies' outcomes.

All of the examples discussed thus far employ populations of single species, but in nature microbes rarely exist as monocultures. As with most fields of biological study, theory precedes experimental validation, and theory suggests that in populations with multiple species, spatial self-structuring allows the formation of sub-communities that can be differentially adapted and between which natural selection differentiates [77, 101, 102]. One notable mixed-species community that has been examined experimentally is the symbiotic consortium of *Acinetobacter* and *Pseudomonas putida* [67, 93]. Initial studies of these two organisms co-cultured in biofilms demonstrated that *Acinetobacter* can metabolize benzyl alcohol to benzoate which leaks out of the cells of this population and can be metabolized by *P. putida*. An emergent structure arose in the mixed-species

biofilm after a few days; *P. putida* formed a mantle over *Acinetobacter* microcolonies. Next, some *Acinetobacter* microcolonies began to grow in the aerial regions of the *P. putida* structure, close to the bulk medium which was the source of benzyl alcohol [67]. This spatial arrangement optimized collaboration in benzyl alcohol degradation between the two species, allowing them to coexist in environments with lower benzyl alcohol concentrations than would normally support their coexistence [93]. By observing changes in colony morphology of *P. putida*, the emergent structure was found to be correlated to a change in colony phenotype, which was traced to a genetic polymorphism in the strain [93].

The simplicity of the *Acinetobacter* and *P. putida* experimental system enabled identification of causality: the spatial structure of the environment afforded the community an opportunity to organize spatially which, in turn, allowed the rise of mutations that were beneficial to the symbiosis. Although these authors identified emergent structure in the symbiotic consortium, and propagated individuals engaging in it to new environments, they did not propagate the actual structure to new environments. Given time, the individuals could re-establish the emergent structure, but it might be interesting to see how propagating pre-organized pieces of the structure to new environments would impact the fate of the consortium. Large pieces of physical structure are routinely conserved between biofilm environments by the propagation of aggregates, suggesting that biofilms might be a good place to look for evidence of community evolution.

### **3.4 Background: Physical structure of biofilms**

#### **3.4.1 Origins and evolution of biofilm structure**

Within biofilms everything from species composition to cell density, and from gene expression to cell morphology, can vary by location and through time [69, 82, 103]. The physical structure of a biofilm is the result of a constant conversation between these cell- and population-dependent variables, and variables present in the physical environment such as temperature, pH, and dissolved oxygen concentration [104]. Biofilms may represent an important transition between uni- and multi-cellular life [76, 84, 94, 105, 106]. Evidence pointing to this includes the fact that bacteria commonly undergo gene transfer in biofilms [107-109]; the pool of available sequence space is larger than just the set of neutral or beneficial mutations available to the genome of the individual. Furthermore, bacteria exhibit direct metabolic interactions with one another even in laboratory biofilms, and proximity and community composition influence these types of interactions [110].

The formation of heterogeneous physical structure in biofilms hints that natural selection acts at the community level [77, 97]: the drive of individual cells to optimize their own access to nutrients while protecting themselves from environmental threats must play a role in determining biofilm structure [104], but some cells must sacrifice by colonizing the substrate, where access to nutrients is limited, in order to provide others with opportunity [105]. In other words, while it is detrimental to individual cells to become the basement layer in a biofilm, it is beneficial to the community to adhere and thereby to remain in an environment that supports life. The presence of surface colonizers cannot necessarily be predicted without knowledge of the higher level of

organization. The inclusive fitness conferred by surface-adhesion genes outweighs the costs associated with their expression.

Beyond the evolutionary origins of biofilms, thinking about evolution of biofilms and their structure requires us to think not only of the immediate environment in which the biofilm is found, but also of the global environment. The cells in a biofilm that are most likely to access nutrients are those that reach out furthest from the substrate into the environment, but these are also the most likely cells to be removed from the biofilm in the presence of flow. From the perspective of the immediate biofilm, the cost of being removed from the environment (essentially, death) outweighs the benefit of acquiring a small (not life-or-death) nutrient advantage. However, while the displaced cells “die” in the immediate environment, they can potentially be the first cells to colonize downstream environments. Therefore, their genes are propagated in a global sense and the inclusive fitness of the ability to leave a biofilm in search of new environments can be a net positive. Here is a potential example of Simpson’s paradox: although the ability to “leave” a biofilm compromises the accumulation of “leavers” on a local scale, “leavers” will dominate on a global scale as long as they can colonize downstream environments as efficiently as “nonleavers” can [111, 112]. We will return to this theme later.

### **3.4.2 Development, composition, and propagation of biofilm structure**

Most bacteria on earth can form biofilms, as can many other micro-organisms. Naturally occurring biofilms usually contain a mix of species, and environmental fluctuations can impact every species, or even each individual, differently [106, 113]. Mixed population biofilms can exhibit very different dynamics than their planktonic counterparts. For

example, neither planktonic growth rates nor monoculture biofilm growth rates accurately predict the growth rates exhibited by *Burkholderia cepacia* and *Klebsiella oxytoca* when both species are cultured together in a biofilm [114, 115]. Thus, it is virtually impossible to predict, *a priori*, what the structure of a particular biofilm will look like in a particular environment. Even if all controllable variables are known, stochastic fluctuations in the environment and in gene regulation can dramatically affect biofilm structure [104]. As a result of these uncertainties, most studies about biofilm structure are descriptive and not prescriptive, and many are qualitative [116].

Researchers most often use confocal laser scanning microscopy (CLSM) to study biofilms, but small pH and oxygen sensors can provide additional information about conditions within biofilms, fluorescent reporters can convey metabolic information [69], and staining cells and exopolysaccharides can provide endpoint information about biofilm composition [117]. Some efforts to quantify biofilm structure have been made, and the standard is a Matlab package called COMSTAT that calculates various metrics for CLSM images of biofilms including biomass and colony size [118].

There are two broad classes of biofilm structure. First, biofilms can be flat and monomorphic, although this is unusual in natural biofilms. In *Escherichia coli* the deletion of genes related to surface adhesion and cell–cell aggregation can cause flat structure under certain environmental conditions [117]. Deletion of metabolic genes that render a population very unhealthy, lack of cell surface appendages, or severe nutrient limitation, for example the absence of amino acids in the growth medium, can also lead to flat structure in *E. coli* biofilms (observations of present study). Providing citrate as the sole carbon source causes flat structure in usually robust and complex-structured *P.*

*aeruginosa* biofilms [119]. Additionally, in mixed-species microbial biofilms that are isolated from nature and cultured in the laboratory, severe nutrient limitation can cause flat structure [120].

Secondly and more commonly, biofilms can exhibit complex three-dimensional structure. Here, pillars (also referred to as mushroom clouds) of biomass that reach out from the substrate are surrounded by invaginations, tunnels, and caves through which liquid can flow or diffuse to deliver nutrients and remove waste products. Biofilms which form three-dimensional structure pass through five cyclical stages: initial adhesion to a surface, active growth, mature three-dimensional structure and/or formation of mushroom-shaped clouds, dispersal from the biofilm, and return to planktonic phase. Initial active growth in a biofilm is clonal, such that distinct clusters of whatever initially stuck to the surface will be observed growing from the point of initial adhesion with little exchange of biomass between these clusters [116]. Dispersal occurs with the greatest frequency after significant biomass has accumulated on the substrate. Then, single cells detach or are divided away from the biofilm to become planktonic, and large chunks—aggregates—of biofilm spontaneously detach and move downstream. We will return to a discussion of aggregates, but let us first examine observations of biofilm structure.

### **3.4.3 Development of structure in monoculture biofilms**

*Bacillus subtilis* is a spore-forming bacterium that exhibits a coordinated structure, which is referred to as a colony biofilm, when colonies are grown on solid media. In one study *B. subtilis* colony biofilms were cultured on agar surfaces and the authors monitored expression of three different genes, whose expression indicates three separate

physiological states, with fluorescent reporters [121]. The study found that most cells were motile early in biofilm development, while midway through biofilm development most motile cells stopped producing motility genes and began to express a high amount of extracellular matrix. Cells expressing the most matrix were distributed in patches throughout the height and width of the biofilm and were theorized to provide the structure with integrity. Late in biofilm development some matrix-producing cells, particularly those in the aerial regions of the biofilm, began expressing spore-formation genes. Overall, this study demonstrated that a monoculture biofilm can exhibit complex differentiation through time and space because of coordinated gene expression [121].

*P. aeruginosa* is a common model organism for biofilm studies. One study demonstrates, much like the study of *B. subtilis* just described, that *P. aeruginosa* differentiates through space and time within biofilms based upon coordinated gene expression [122]. Using gene deletions and chemical treatments, the authors determined that expression of cell-surface appendages and chemotaxis-related genes, as well as quorum-sensing controlled release of DNA from cells, are required for formation of mature biofilm structures, including the caps on top of mushroom-shaped clouds [122]. Unlike the study of *B. subtilis*, the authors found that cells in the aerial regions (caps) on *P. aeruginosa* biofilms were more likely to contain motile cells, and that instead of progressing through every lineage, motile cells are present from the start of biofilm formation but swim up the mushroom stalk, via chemotaxis, to form the cap late in biofilm development [122]. These studies of *B. subtilis* and *P. aeruginosa*, taken together, demonstrate not only that differentiation occurs in monoculture biofilms, but also that no one species can be used to predict how another will act in a biofilm.

Members of different species form and populate three-dimensional biofilm structures dramatically differently in time and space, even when the overall biofilms exhibit similar three-dimensional architectures.

*P. fluorescens* is another well-characterized biofilm-forming strain that is commonly used in laboratory studies [87, 88, 97, 98]. When *P. fluorescens* is grown in spatially heterogeneous environments, such as stagnant liquid culture, genetic polymorphisms arise and different morphs, whose phenotypes are easily observed because of variations in colony morphology, populate different niches in the culture [87, 88]. After morphs arise, if the culture is sampled and samples are returned to a homogeneous environment (shaken liquid culture), the morphs revert to wild-type. As this study highlights, *P. fluorescens* is a model organism for adaptive radiation. Both *P. fluorescens* and *P. aeruginosa* are also used in laboratory studies of community evolution, as described in the previous background material, because both exhibit cooperative behavior that can be interrupted by the rise of cheats.

#### **3.4.4 Aggregates in structure propagation and evolution: Simpson's Paradox**

Aggregates up to 500  $\mu\text{m}$  in diameter have been observed to detach from and move downstream in laboratory biofilms during detachment phases [123], but such large aggregates are unlikely to be found in our biofilm flow system given the dimensions of the flow chamber and tubing that we use. It is more likely that we see aggregates averaging between 50 and 60  $\mu\text{m}$  in diameter in our system [123]. Aggregates do not usually include the biomass from the substrate [123]. As a result, whatever cells initially colonize the substrate are likely to stay there, while detaching clusters will contain a

mixture of whichever cells inhabit layers of the biofilm above that basement layer [123]. This indicates that cells which grow away from the substrate faster will be more likely to detach in aggregates, and more aggregates will shed from biofilms that are able to accumulate more total biomass.

Once aggregates detach, they will either roll along the surface of the biofilm with potential to reattach to the same biofilm downstream, or leave the biofilm entirely to move downstream and potentially colonize a virgin surface [123]. Aggregate propagation may be a key mechanism by which a single type of biofilm structure takes over in a given environment. Aggregates can also convey mixed-population biofilms between environments. This second observation has important implications when examining the evolution of microbes in biofilms and perhaps of microbes in general. Because aggregates are pieces of biofilm within which cells may be pre-organized in an optimal physical structure, cells within them may work together more efficiently once they reach new environments than do naïve cells coming together for the first time. Thus, the inclusive fitness conferred by genes that cause mixed populations to form stable mixed-species structures may be higher than the inclusive fitness of genes that bolster the growth of individual cells. In other words, although theory and some experiments suggest that the primary benefit of three-dimensional structure formation is optimal growth and nutrient acquisition for individuals in a given environment [69, 124, 125], or protection for individuals from anti-microbial treatments [86, 126, 127], three-dimensional structure may be equally important as a mechanism that promotes optimal downstream colonization by the whole community via aggregate detachment and downstream re-attachment.

This suggests a corollary. Hypothetically, since most bacteria on earth exist as biofilms, evolution of bacteria must be seen in light of the growth opportunities afforded by biofilms. If biofilm growth renders individuals less fit than aggregates to colonize downstream environments, the force of natural selection should yield individual bacteria that are optimized to interact with their community rather than individually most fit. Communities of bacteria can become symbiotic, even at the expense of individual fitness of community members, if symbiosis allows the community to dominate on a global level. Put another way, Simpson's Paradox predicts that individuals that are locally less fit can still be globally more fit, explaining the maintenance of apparently less-fit populations in local communities [111, 112]. One study using co-cultures of engineered cooperating and cheating strains of *E. coli* (which were grown without explicit physical structure in shaken liquid cultures) demonstrated Simpson's paradox. Even though cooperators grew more slowly, and therefore became a smaller fraction of their local populations in every instance, the populations that initially contained more cooperators grew better overall so that the global ratio of cooperators to cheats increased [111].

But does all of this speculation have any basis in reality? Do communities of symbiotic bacteria form structures that optimize cooperation? If so, can such structures be propagated to new environments by aggregates? If so, does having this pre-arranged structure confer any advantage to the community in its new environment? These are the questions we attempted to address in the present study.

We designed an engineered symbiotic ecosystem to explore its structure and function. It is plausible that adhesion and aggregation genes could be "lost" to some subpopulations in a stable biofilm community, if one subpopulation is primarily

responsible for cohesion of the overall biofilm and others come to depend upon the biofilm formation ability of the first. In our engineered system, one population has lost significant clusters of genes implicated in adhesion and aggregation so it depends upon the other population for biofilm formation. However, the biofilm-forming population is metabolically compromised and it forms only weak monomorphic biofilms alone. Its metabolic deficiency, and therefore its capacity to grow and form healthy biofilms, is compensated only in the presence of the biofilm-deficient population. We wanted to see, first, if this engineered symbiotic consortium would survive, how stable its function would be, and whether any discernable nonrandom three-dimensional structure would arise in the symbiotic biofilm. When we found that a particular three-dimensional structure did repeatedly emerge, we sought to determine whether it could be inherited by downstream communities. It could be inherited, and its presence was correlated with the presence of aggregates in the set of propagated cells. A growth advantage was also inherited by downstream communities that inherited these aggregates. Before turning to our results, let us put our study in perspective by examining what others have discovered about structure in microbial communities using engineering techniques.

### **3.4.5 Engineering approaches to studying microbial structure**

The *Acinetobacter* and *P. putida* experimental system, described above, provides an entrée into a survey of how engineering techniques have been used to explore physical structure in microbial communities. That symbiotic system is natural in that the strains were not engineered, but it is synthetic in that these two strains do not necessarily coexist in nature. In another study of a natural-but-synthetic ecosystem, the authors used a

microfluidic device to simulate a spatially heterogeneous environment. Using it, they were able to culture a three-member community of soil bacteria [91]. Coexistence of multiple competing species can require persistent, self-organized, spatial arrangement [102] and this, in turn, can depend upon the natural environment in which the community originates. It is difficult to mimic complex natural environments in the laboratory, but microfluidic devices have the potential to come close. The three-member community cultured in this study, which is representative of similar communities found in nature, could not coexist in bulk medium, nor could any of the members grow alone. However, when the three populations were kept isolated but within several hundred microns from one another in the microfluidic device, and were allowed to communicate with one another through microfluidic channels, all three species survived and grew [91].

Several studies have examined physical structure in *E. coli* communities. A study employing microfluidic devices observed growth of *E. coli* in small, structured spaces that were perfused with nutrients [90]. The authors observed that the cells quickly self-organized to orient their long axes in parallel with the primary direction of nutrient diffusion, and they used computational models to confirm that the average shape and size of an *E. coli* cell is well adapted to colonizing small spaces while maximizing diffusion to the interior of the colony [90]. Yet another study also examined a community of *E. coli*, here with three different strains that compete in a canonical rock-paper-scissors ecosystem (one beats the second, who beats the third, who beats the first) [89]. The authors used simple plate-based culturing techniques to demonstrate that the three strains coexist when interactions are constrained to occur over only a local region, whereas the strains cannot coexist when cultured in the well-mixed environment of a shaken flask

[89]. A final study examined two competing polymorphic populations of *E. coli* in a microfluidic environment and discovered that isogenic aggregates of each population formed after co-culturing [92]. The formation of these aggregates was not dependent upon competition, but was a feature of the *E. coli* themselves. The authors suggest that selection is operating at multiple levels, including upon the physical structures present among bacteria in the microfluidic device, to promote fitness of both genotypes despite the competition between them [92].

Here, we present a synthetic symbiotic consortium in which two populations of *E. coli* depend upon one another for survival in biofilms. The first population cannot synthesize lysine but can form biofilms. The second population cannot form biofilms alone, but it can synthesize lysine and can activate lysine production in the first population. This consortium exhibits emergent structure, and we find that when aggregates of cells from initial biofilms are propagated to downstream biofilms, the emergent structure and a growth advantage are transferred also.

### **3.5 Design and construction of the symbiotic consortium**

#### **3.5.1 The biofilm-forming, but metabolically deficient, population**

The symbiotic biofilm consortium consists of two engineered populations of *E. coli* MG1655, one of which is deficient in biofilm formation but otherwise healthy, while the other is metabolically compromised but capable of biofilm formation (Figure 3.1). To compromise metabolism in strain MG1655, we interrupted the biosynthetic pathway for lysine and diaminopimelate by deleting *dapD*, the gene encoding tetrahydrodipicolinate N-succinyltransferase, creating strain MGd- [128]. *DapD* was then replaced on an

engineered plasmid under control of the transcriptional regulator RhIR, which is activated by the small, freely diffusible acyl-homoserine lactone (acyl-HSL) butanoyl-homoserine lactone (C4HSL) [61]. This strain was marked by constitutive expression of eCFP, and will be called the blue population.

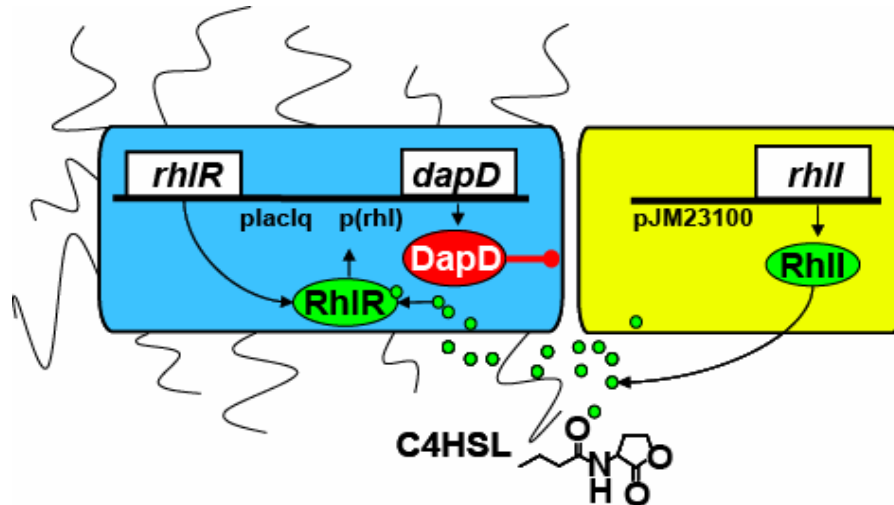


**Figure 3.1** The synthetic symbiotic consortium. Two populations of *E. coli* coexist because they communicate. The blue population cannot synthesize diaminopimelate or lysine but can form biofilms. When grown as a biofilm in the absence of lysine or diaminopimelate, this population forms a scant biofilm that eventually dies. The yellow population cannot form biofilms alone, but it is otherwise healthy and it synthesizes a small molecule, C4HSL, that activates lysine production in the first population. Yellow cells cannot form biofilms unless they are bound within the biofilm formed by the blue population. Only when these two populations are grown together can they form viable biofilms that persist.

The engineered plasmid in the blue population was constructed from pFNK202 which encodes constitutive expression of *RhIR* [42]. Proper function of the symbiotic consortium requires that very little DapD be present in blue cells in the absence of the yellow population, while the presence of yellow cells should restore biological levels of DapD to blue cells. However, minor expression (promoter “leakage”) of DapD allows the blue population to begin forming a sparse biofilm without C4HSL so that the symbiotic consortium can gain a foothold in the environment. We obtained an adequate

basal expression level of *dapD*, with wild-type levels of biofilm formation in the presence of saturating C4HSL, by placing *dapD* under control of the RhIR-activated promoter p(qsc119) with ribosome binding site (RBS) H, and attaching an LVA degradation tag to DapD. We tried various other permutations of this arrangement, including a variety of RBS strengths, and expressing *DapD* with and without the LVA tag, but this combination yielded optimal behavior.

### 3.5.2 The biofilm-deficient (but healthy) strain

To construct a biofilm deficient version of MG1655, we deleted three groups of genes that are implicated in biofilm formation. First, a primary determinant of both initial adhesion and three-dimensional structure formation in *E. coli* biofilms is the presence of the cell-surface appendage called curli. Curli can be seen in scanning and transmission electron microscope images as fibrous bundles protruding from and swirling around the cell wall of bacteria, and the curli of adjacent cells appear to intertwine. Curli are important for initial adhesion to abiotic surfaces [129] and also for cell-cell adhesion that leads to three-dimensional structure formation [117, 130]. In *E. coli*, curli are optimally expressed at 30°C under low nutrient and low osmolarity conditions [131, 132], which are similar to the conditions we use in our study. When *csgA* and *csgD* were deleted from *E. coli* in previous studies that used similar conditions to our study, a sparse monolayer was the best biofilm formed by the resultant strain [117].

Two operons, *csgDEFG* and *csgAB*, are responsible for the biosynthesis of curli monomers (CsgA) and their export. We deleted both operons entirely. One of the deleted genes, which is involved in regulation of curli expression, expresses a RhIR

homolog, CsgD [129]. It is not clear whether CsgD can either interact with C4HSL or bind the p(qsc119) promoter that we used in the engineered plasmid for the blue population, but its absence could potentially alter the effect of C4HSL upon the biofilm-deficient population relative to the blue population.

A secondary factor, which is involved in strong surface adhesion of *E. coli* biofilms but not as clearly involved in the formation of three-dimensional structure, is the presence of type I pili (also called fimbriae). These cell-surface appendages form catch bonds whose binding is characteristically tighter under higher stress [133, 134]. Genes responsible for fimbriae lie in the *fimA–fimH* locus, and the key gene whose product mediates catch bond formation is *fimH*. We used a mutant lacking the entire locus for the purposes of this study [133]. Many experimental studies use mannose-BSA to provide for catch-bond formation. Here, we used bovine ribonuclease B quenched with bovine serum albumin (BSA). In single mutants lacking the *fim* locus, we observed significantly less initial adhesion than in any other single mutant that we made.

A third factor, implicated in three-dimensional structure formation of *E. coli* biofilms but not in initial adhesion, is the presence of colanic acid (CA) [117]. CA is an excreted polysaccharide that surrounds cells in biofilms and creates space between them which presumably allows for diffusion of nutrients and wastes, for communication between cells, and for growth. CA is a constituent of the “slime” that is commonly mentioned in macroscopic observations of biofilms. It is not clear whether *E. coli* MG1655 produces CA when it is sessile [117], but CA is probably important in determining the initial three-dimensional structure of MG1655 biofilms while cells are actively growing and dividing. Both theory and experiments indicate that biofilms of

cells lacking the genes encoding CA are flatter and cells are more tightly packed [117, 135]. 19 genes in the *wca* locus are responsible for CA production and secretion. Genes encoding CA are most highly expressed at temperatures below 25°C and in minimal medium with an accessible carbon source [136]. These conditions are approximately those in our study so we deleted the entire locus *wcaL–wza*.

Many other gene products also influence the structure of *E. coli* biofilms. For example, when *E. coli* have the F plasmid that provides conjugative machinery, they exhibit better initial adhesion and also more prominent three-dimensional structure under conditions where medium is constantly refreshed but there is no clear pattern of flow [137]. The pilus structure expressed from the F plasmid seems to promote nonspecific cell–surface and cell–cell adhesion [137]. In contrast, under conditions more similar to those in our study, constant flow in a biofilm chamber, the F plasmid does not significantly enhance initial adhesion but it does contribute to the formation of three-dimensional structure [116]. The strain we used, MG1655, does not have the F plasmid or any conjugative machinery; this protects our two populations from exchanging the genetic material with which we programmed them.

Other genes that may contribute to biofilm formation in *E. coli* under some conditions include *flu*, which encodes a cell-surface autotransporter called antigen 43, and *flhD* and *flhC*, master regulators for the expression of flagellar genes. All three of these genes have been shown to be particularly important in biofilm development at 37°C [138, 139]. However, we made single, double, and triple mutants of the *fim* locus, *flu*, and *flhDC* and found that neither  $\Delta flu$  nor  $\Delta flhDC$  significantly reduced biofilm formation under the conditions that we use when  $\Delta fim$  was present (data from

observation). In fact, one or both of these deletions may actually enhance biofilm formation under the conditions we use (data from observation). The study which identified these genes as important did use biofilm flow chambers, but they did not coat the chambers with bovine ribonuclease B, they maintained the biofilm at 37°C rather than 30°C, they allowed a much longer time for initial adhesion (2 hours) than we do (5 minutes), and they flushed the chambers after incubation with a much higher flow rate (0.8 mL/min rather than 0.2 ml/min, which we use) [138]. This demonstrates how difficult it is to predict biofilm formation, and highlights the dramatic impact that environmental variables can have upon gene regulation and thereby upon biofilm formation.

Finally, strain MGfwc- was constructed from MG1655 lacking the curli locus ( $\Delta csgC-csgG$ ), the type I fimbriae locus ( $\Delta fim$ ), and the colonic acid locus ( $\Delta wcaL-wza$ ). This population contained an engineered plasmid encoding strong constitutive expression of the C4HSL synthase, RhII. This engineered plasmid was constructed from pFNK102 [42]. Yellow cells must synthesize enough C4HSL to activate RhIR, and thereby to upregulate *dapD* expression, in the blue population early in the lifespan of the consortium so that the blue population does not die. The strong constitutive promoter J23100 combined with RBSII yielded enough C4HSL in the biofilm environment to activate the symbiotic function. The strong constitutive promoter p(lacIq), even coupled with RBSII, did not provide adequate C4HSL production to enable optimal function of the symbiotic consortium. This strain contained a YFP marker plasmid, and is called the yellow population. More information about the construction of both strains can be found in Methods and in Appendix B.1.

## **3.6 Function and stability of the biofilm consortium**

### **3.6.1 Initial characterization of the function of the symbiotic consortium**

To confirm that the symbiotic consortium functions as designed, we inoculated a 50/50 mixture of blue and yellow cells into biofilm flow cells alongside separate control monoculture biofilms of each population. No yellow biofilm was observed in the yellow control monoculture and the blue control monoculture formed a scant biofilm alone (Figure 3.2A). Only a small fraction of the yellow population remained in the mixed biofilm after 24 hours of growth, confirming the inability of yellow cells to form biofilms, but as the mixed biofilm matured it accumulated significantly more biomass than either control (Figure 3.2A). By 96 hours, the yellow population recovered to constitute half the total biomass, and that balance remained stable until after 120 hours (Figure 3.2B). This answered our first question: the engineered microbial consortium survived and grew. Next, we wondered how stable this coexistence and cooperation would be.

### **3.6.2 Stability of natural ecosystems**

There are many theories about what makes natural ecosystems stable, but there are very few demonstrations of ecosystem stability that involve microbial ecosystems. One theory suggests that asymmetries in how dependent species are upon one another's presence, when coupled with differences in fitness, can lead to maintenance of species diversity in communities. This is true for some plant-animal mutualistic networks [140]. But a study

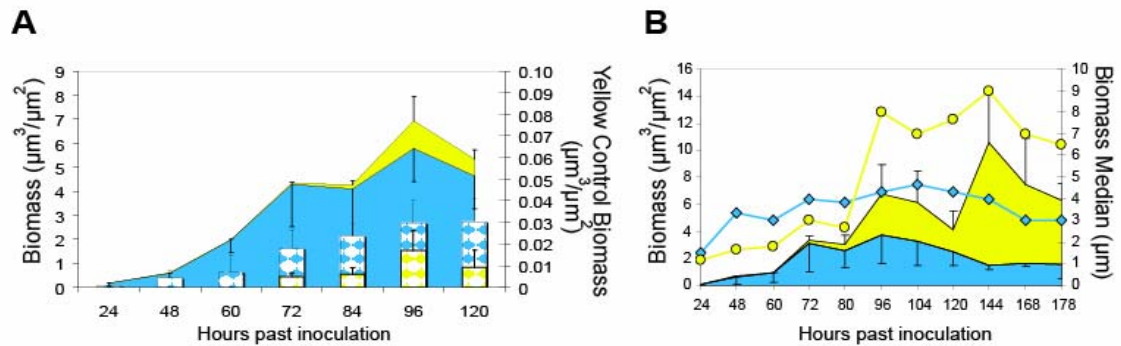


**Figure 3.2** Initial characterization of the symbiotic consortium. (A) The symbiotic consortium functions as designed. The blue population control forms a biofilm which eventually dies, and the yellow population accumulates no biomass before 72 hours, and very little biomass over the lifespan of the experiment. When the yellow and blue populations are inoculated in a 50/50 mixture, significantly more biomass accumulates than when either population is inoculated alone. (B) The consortium functions when grown for long periods of time. At first the yellow population is a strict minority but by 96 hours it constitutes half the biomass of the consortium. Between 80 and 96 hours the yellow population shifts to accumulate primarily above the blue population. (Solid yellow areas, yellow biomass in consortium; solid blue areas, blue biomass in consortium; blue bars, blue control biomass; yellow bars, yellow control biomass plotted against right axis; yellow line, biomass median of yellow population; blue line, biomass median of blue population. All errors are standard deviations.)

by LaPara et al. challenges this theory [22]. Here, when a natural community taken from a waste-water treatment plant was subjected to decreasing nutrient concentrations, 16s rRNA and rDNA analyses revealed that while functions were conserved in the community, redundant populations were eliminated. Survival of this natural community occurred because of diversity, but also at the expense of diversity.

A second body of theory postulates that taxonomic diversity is the fundamental determinant of community stability [141]. Kiessling surveyed reef ecosystems and found that taxonomic diversity is related to ecological stability on evolutionary timescales [142]. However, studies on shorter times-scales do not agree with this theory. Rather, on shorter time-scales, a third body of theory claims that functional diversity within communities dictates invasibility and community stability. In other words, the more survival strategies that a community can try when it encounters stress, regardless of who tries them, the more likely it is that the community will survive. The study explicated

above by LaPara et al. supports this theory [22], but in one dissenting view Arenas et al. surveyed communities of algae and determined that specific species identities, rather than functional diversity, determined resistance to invasion [23]. The number of populations of algae considered by Arenas et al. was very small ( $< 4$  species) so broad application is questionable.

Experimental evidence lags theory about ecosystem stability because naturally occurring symbiotic communities are difficult to culture in the laboratory. In a simple sense, our engineered symbiotic ecosystem exhibits behavior consistent with the third theory. That is, the presence of both engineered populations enables the entire community to survive in a biofilm and under nutrient stress, whereas neither population could do so alone.

### **3.6.3 Stability of biofilms in nature**

There is much evidence that the biofilm mode of growth confers resistance to antimicrobial chemicals [126, 143]. Additionally, biofilm communities in nature are stable over periods of time on the order of years, even as the species balances fluctuate within that time in response to nutrient availability, temperature, and light (seasonal variance) [144-146]. Furthermore, evidence from geomicrobiology suggests that microbial communities may exist and perform their functions over evolutionary timescales [147]. Biofilm communities composed of species found in nature, but cultured in the laboratory, can be stable for periods of several weeks or months [36, 123] but there is little experimental work regarding the stability of engineered multi-species populations in biofilms.

### 3.6.4 Stability of the engineered symbiotic biofilm consortium

We observed that the symbiotic biofilm ecosystem was stable, both populations continued to co-exist, for up to 288 hours after inoculation (the experiment was terminated at that point). During this time, the biofilm exhibited oscillations in total biomass characteristic of biofilm growth and detachment/sloughing phases (see section on biofilm structure for a description of these phases), and the timing of these phases was remarkably repeatable in independent biofilms that were grown months apart [analysis of variance, ANOVA,  $F_{0.05}(3,28) = 0.47 < F_{\text{crit}} = 2.947$ ,  $P = 0.70$ ] (see also Appendix B.2). In no case did either population die off during the length of the co-culture experiment.

Additionally, the blue and yellow populations function as designed—the yellow population does not recover wild-type biofilm forming ability and the blue population does not grow without exogenous C4HSL—for at least 288 hours in the biofilm, and during this time the engineered plasmids also remain unchanged (data from sequencing and observation). This was somewhat unexpected; we thought an engineered biological system, particularly under the selective pressures of biofilm growth in minimal medium, would mutate to escape engineered control much more quickly. This result begs for further experimentation to determine whether engineered consortia are more stable than engineered monocultures [1, 148]. However, it has been shown that although engineered control can be lost in *E. coli* within 70 hours in batch culture, control is retained over a period of 200 hours when the same monoculture is grown in a micro-chemostat [149]. It is not entirely surprising that the biofilm environment might afford an equal opportunity. This answered our second question: the engineered symbiotic consortium was stable over at least a period of 12 days.

### 3.7 Physical structure in the engineered symbiotic consortium

#### 3.7.1 Initial observations of structure

We explored the physical structure of the mixed biofilm by calculating the biomass median for each population at each time-point (Figure 3.2B). The biomass median is an indicator of the location of individual populations with respect to the substrate in mixed biofilms; 50% of the biomass of a given population is located between the substrate and the biomass median of that population. If a population has a larger biomass median, its biomass is primarily localized away from the substrate, whereas a population with a smaller biomass median grows close to the substrate. The minimum biomass median (1  $\mu\text{m}$ ) indicates that most cells in the population are attached to the substrate (see also Appendix B.3). Between 80 and 96 hours of growth a significant shift occurred in the symbiotic consortium; although there was still more blue biomass than yellow, the yellow population moved from below or within the blue population to a position significantly further from the substrate than the blue population (Figure 3.2B). Observations corroborate this distinct phenotypic change—clumps of yellow biomass form a mantle over the blue biomass (Figure 3.3).

We identified this change in the symbiotic biofilm consortium as emergent structure, reminiscent of the structure that arose between *Acinetobacter* and *P. putida* in studies described above. It is interesting to note that our results stand in contrast to results generated in one theoretical paper [135]. There, the authors used computational modeling to predict three-dimensional structure in a mixed biofilm containing two populations: extra-cellular matrix producers (like the blue population in our study), and

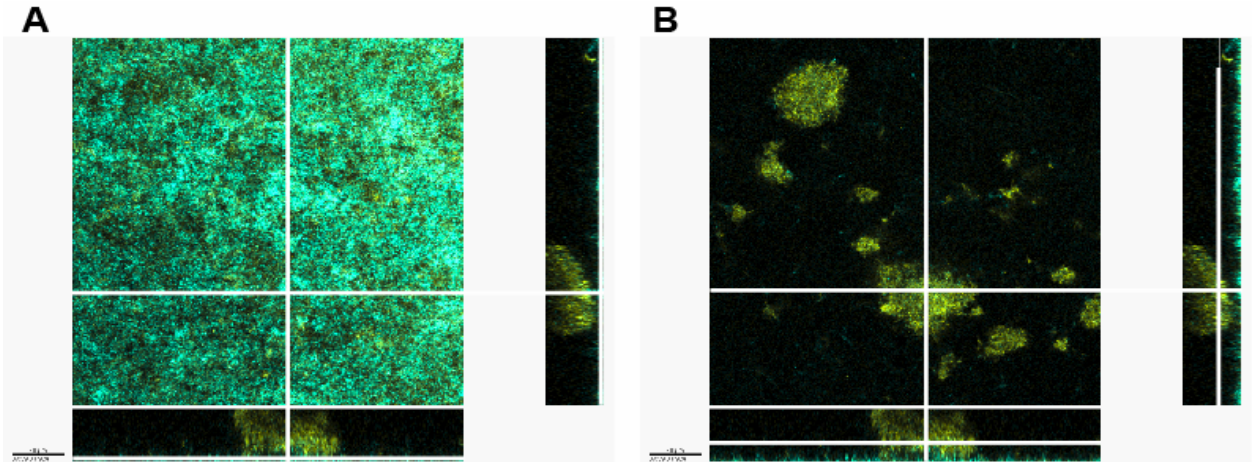


**Figure 3.3** Projections showing emergent structure in a 38  $\mu\text{m}$ -thick symbiotic biofilm. (A) After 96 hours of growth, the consortium exhibits emergent structure. The blue population grows primarily near the substrate, as shown in this projection that is taken at the level of the substrate. (B) The yellow population forms clouds on top of the blue population, as shown in this projection taken at 1/3 the total height of the biofilm, above most of the blue biomass.

nonproducers (like the yellow population in our study). In the outcome of that model, the producers formed bulbous structures very similar to the ones we observe to be formed by our nonproducers (our yellow population) on top of a flat, nonproducer biofilm. This is exactly the opposite of the emergent structure that we observe. A direct comparison between our experiments and their model cannot be made because of the additional mutations which we introduced into strain MGfwc-; however, it is still an interesting juxtaposition. Overall, this result answered our third question: a discernable, nonrandom, repeatable structure emerged in the co-culture biofilm of the symbiotic consortium. Did the structure appear in downstream environments more quickly than it initially emerged in this first generation?

### 3.7.2 Exploring the transfer of the emergent structure

In biofilms, initial growth is clonal, but cells later detach from the biofilm and move downstream to populate new environments [116]. Under these conditions, a given clone or community can be selected if it grows away from the substrate most quickly, detaches to move downstream first, adheres, and grows best in the downstream environment. We wondered whether the emergent structure observed in the symbiotic biofilm could be transferred to downstream environments, and whether it was related to a growth advantage there. We simulated a population bottleneck by propagating two samples into fresh flow cells: one from a 48-hour-old consortium, before the emergent structure appears, and one from an 80-hour-old consortium exhibiting emergent structure. In both cases, the number of cells transferred was the same.

When the 48-hour-old consortium was propagated, the second-generation biofilm accumulated less biomass than the blue monoculture control (from Figure 3.2A). Presumably, early propagation transfers an immature community in which the blue population is sessile or dying as it awaits recovery of the yellow population. However, when the 80-hour-old consortium was propagated, biomass medians of the second generation revealed that the emergent structure was transferred to the second generation: within 48 hours the yellow biomass was found significantly further from the substrate than the blue biomass (Figure 3.4A). This answered part of our question: once established, the emergent structure could re-establish much more quickly in a downstream environment. But would the downstream biofilm have any advantage over a biofilm that began with naïve cells?

### **3.7.3 The second generation has an advantage**

We observed that the second generation biofilm exhibited a growth advantage over the first generation. It formed a biofilm far more quickly: after 48 hours of growth, second generation consortia accumulated an average of 15 times, and as much as 30 times, the biomass accumulated by first-generation consortia in their first 48 hours [ANOVA  $F_{0.05}(3,4) = 0.358 < F_{crit} = 6.591$ ,  $P = 0.78$ , see also Appendix B.4]. Not only did the second generation accumulate biomass more quickly, but it also accumulated more total biomass. After 48 hours of growth, the average total biomass of the second generation was double the average of the highest ever recorded first-generation biomasses (Figure 3.4A, see also Appendix B.4). Overall, when the symbiotic biofilm consortium is mature, it exhibits emergent structure which can be transferred to downstream environments. Additionally, the downstream biofilm consortium exhibits a growth advantage, consisting of faster and greater total accumulation of biomass, over the initial consortium. These results raise two further questions: first, how is the emergent structure transferred? Second, why is there a growth advantage in the second generation?

## **3.8 Aggregates in the transfer of emergent structure and growth advantage**

### **3.8.1 Aggregates and emergent structure**

Evidence suggests that aggregates can detach from mature biofilms and seed downstream communities [123]. To evaluate the role of aggregates in the transfer of the emergent structure between generations, we performed the propagation experiment described above but treated the first generation to break up multi-cellular structures before inoculating it

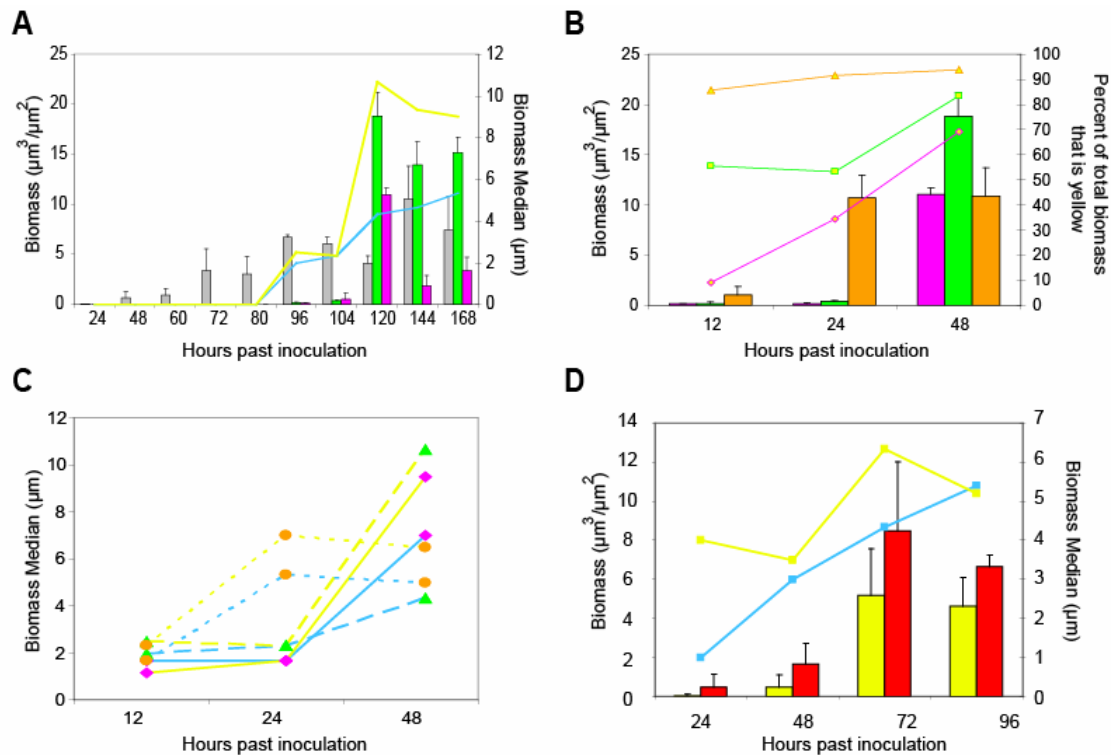


**Figure 3.4** Biomass comparisons between generations. (A) Both second-generation consortia accumulate biomass more quickly than the first generation. The untreated second-generation accumulates biomass more quickly and accrues more total biomass than either the first- or treated second-generations. The biomass medians (plotted against the right axis) of the untreated second-generation indicate that the emergent structure is present. (Grey bars, first-generation biomass; green bars, untreated second-generation biomass; pink bars, treated second-generation biomass; blue line, biomass median of untreated blue population; yellow line, biomass median of untreated yellow population.) (B) The treated and untreated consortia start with the same amount of total biomass, but the treated biofilm has only 10% yellow biomass whereas the yellow population constitutes 50% of the starting biomass of the untreated second-generation biofilm. Yellow biomass comprises significantly more than 50% of the second- and third-generation biofilms after 24 hours (yellow biomass percentages plotted against right axis). Total biomass accumulation for the treated second- and the untreated third- (propagated from the treated second-) generations was equivalent after 48 hours, whereas total biomass accumulation for the untreated second-generation was double that total. (Pink bars, treated second-generation biomass; pink line, percentage yellow in treated second-generation; green bars, untreated second-generation biomass; green line, percentage yellow in untreated second-generation; orange bars, third-generation biomass; orange line, percentage yellow in third-generation.) (C) The biomass medians of the treated second-generation populations diverge less than those corresponding to the first-generation (see Figure 3.2B) and untreated second-generation populations (shown here). The biomass medians of the third-generation populations parallel one another and stay low, indicating that the emergent structure is not present. (Solid yellow line, biomass median of treated second-generation yellow population; solid blue line, biomass median of treated second-generation blue population; long-dashed yellow line, biomass median of untreated second-generation yellow population; long-dashed blue line, biomass median of untreated second-generation blue population; short-dashed yellow line, biomass median of third-generation yellow population; short-dashed blue line, biomass median of third-generation blue population.) (D) The YFP+ fraction was able to form a biofilm, but the aggregate fraction biofilm formed most quickly and accumulated the most total biomass. Biomass medians from the aggregate biofilm reveal that the emergent structure is present from the start, and that both populations grow away from the substrate together. (Yellow bars, biomass of YFP+ fraction biofilm; red bars, biomass of aggregate fraction biofilm; yellow line, biomass median of aggregate fraction yellow population; blue line, biomass median of aggregate fraction blue population. All errors in this figure are standard deviations.)

into the second generation (an equal number of cells was inoculated into the first, and treated and untreated second-generation biofilms). We observed that the biomass medians of the blue and yellow populations diverged less in the treated second generation than they did in the first and the untreated second generations (Figures 3.2B, 3.4C). This suggested that the treated second generation did not exhibit the same emergent structure as the first and untreated second generations, but it did not provide conclusive evidence that aggregates convey this structure.

Upon closer examination, we noticed that although the treated and untreated consortia were made from the same inoculum (first-generation effluent), and thus contained the same 50/50 composition of yellow and blue biomass, the treated biofilm had only 10% yellow biomass after 12 hours of growth whereas the yellow population constituted 50% of the 12 hour biomass of the untreated second-generation biofilm (Figure 3.4B). This result indicated that treatment in some way prevented yellow cells from sticking in the second-generation biofilm. We first examined the possibility that treatment damaged the cells. Such damage should have been done to cell-surface structures of both populations and would compromise initial adhesion. However, after only 12 hours of growth, the treated and untreated second-generation biofilms contained essentially equal amounts of total biomass (although, as mentioned above, the fraction of yellow biomass was dramatically different). This suggested that initial adhesion was not compromised in the treated case. Images captured at the substrate after 12 hours of growth in the untreated case show clumps, perhaps aggregates, of blue and yellow cells co-localized on the substrate (see Appendix B.5). In contrast, images of the substrate in

the treated case show clumps of blue cells unassociated with widely dispersed single yellow cells and small yellow clusters (see Appendix B.5).

Given all of these observations combined, we hypothesized that more of the yellow population remains in the untreated biofilm primarily because the yellow cells are aggregated with blue cells. Put another way, sticking to the blue population could help more members of the yellow population to stick and stay in the second-generation biofilm. Further, if the aggregates are pre-organized pieces of the emergent structure, the emergent structure might arise more quickly (as we observe that it does) when the inoculum contains aggregates and it might not emerge at all if the aggregates are disrupted.

### **3.8.2 Aggregates and the growth advantage**

We wondered whether the presence of aggregates in the inoculum conferred a growth advantage to the untreated second generation. While the treated second-generation consortium still grew more quickly than the first generation, it accumulated only half the total biomass of the untreated second-generation consortium in the same amount of time and its maximum total biomass was closer to that of the first generation (Figure 3.4A). This suggested that the presence of aggregates in the inoculum was correlated with at least a portion of the growth advantage—the greater total accumulation of biomass.

### **3.9 Adaptation or polymorphism and the growth advantage**

The observation that some yellow cells were stuck to the substrate after 12 hours of growth in both the treated and untreated second generations is important (see Appendix

B.5). In the untreated second generation, adhesion of yellow cells could be explained if the yellow cells are stuck to the blue cells and the blue cells bring the yellow cells into contact with the substrate. But we observed some single yellow cells and small clusters sticking to the substrate in the treated second generation. We did not observe yellow cells to adhere at all in the first-generation control. This hints at the possibility that an adaptation—perhaps a polymorphism like those described in above sections about *P. fluorescens* biofilms, or a change in gene expression as has been observed in subpopulations of *P. aeruginosa* and *B. subtilis* biofilms—has arisen that makes the yellow population more sticky.

A stickier yellow population could have three effects on the biofilm consortium. First, it could contribute to the emergent structure; as yellow cells become more adhesive, perhaps they form the balls of yellow cells that we observed sticking to one another and to the blue cells in the emergent structure (Figure 3.3). Second, sticky yellow cells might associate more tightly and/or more permanently with blue cells, helping the symbiosis along. Third, sticky yellow cells, if given the opportunity, might disrupt coexistence of the consortium since, being sticky, they no longer need blue cells. We wanted to learn whether the yellow cells had indeed become more adhesive, and to parse the relative contributions made to emergent structure and to the growth advantage by the propagation of aggregates and by the theoretical “sticky adaptation” in the yellow population. Thus, we used cell sorting to separate the yellow cells from the aggregates in the effluent from the treated second generation, and started three third-generation biofilms: a separate biofilm from each sorted fraction, and one control biofilm comprised of untreated effluent from the treated second-generation biofilm.

### **3.10 Third-generation biofilms reveal contributions of adaptation and aggregates**

#### **3.10.1 The control third-generation biofilm**

After 12 hours of growth, the third-generation biofilm consortium control, started from untreated effluent of the treated second-generation biofilm, contained an even higher percentage of yellow biomass than both of the second-generation consortia. Curiously, this third generation initially accumulated biomass faster than any of its precursors (Figure 3.4B). We reasoned that biomass might accumulate faster if yellow cells adapt to grow faster (note that “growth” is a product of cell division whereas “biomass accumulation” results from a combination of cell division and adhesion). If faster growth is the primary adaptation, the yellow biomass should increase at the same rate simultaneously in the treated second generation and in the third generation (which was propagated directly from it) biofilms, because the yellow cells in these two biofilms are clones and nothing happens in the transfer between the generations that should change the rate of yellow cell growth. However, the rate of increase of yellow biomass in the third-generation biofilm was at least seven times greater than that in the treated second-generation biofilm, leading us to conclude that a change in growth rate was not the primary adaptation. Since the yellow cells are metabolically healthy, they grow faster than the blue cells. If they can stick to the substrate and in the biofilm better, yellow biomass, and therefore total biomass, should accumulate much more rapidly, particularly if they are able to colonize more of the substrate in the third generation than in the second. We speculated that the primary adaptation in the yellow cells enabled them to stick more effectively. Importantly, the third generation consortium never accumulated

more biomass than its predecessor, the treated second-generation biofilm, which accumulated only half the total of the untreated second-generation consortium. Additionally, the emergent structure definitely did not reappear in this third-generation control biofilm (Figure 3.4C and Appendix B.6).

From all of these observations, we concluded that at the third generation the yellow cells no longer absolutely require the blue population, so the blue population can be sifted out by population bottlenecks (thus, we see progressively higher proportions of yellow biomass in successive generations). However, this change might be globally maladaptive for two reasons. First, it appears that the consortium cannot accumulate the optimal total biomass without the blue population which is conveyed in aggregates. Second, even though the yellows can stick, they still do not colonize the substrate as effectively as blue cells. From a global evolutionary perspective, the biofilm formed by an inoculum containing aggregates might still be better than the biofilm formed by adapted yellow cells alone. We explored this with biofilms started from separate, sorted fractions of the same effluent that started this control biofilm.

### **3.10.2 Probing adaptation by cell sorting**

We sought to explore biofilm formation by the adapted yellow population and by aggregates separately by using FACS to sort the effluent from the treated second-generation consortium. We gathered two fractions (see Appendix B.7). The first fraction contained single yellow cells (YFP+ fraction) while the second contained aggregates of unknown, assorted size and composition (aggregate fraction). We inoculated these two fractions into separate biofilms. Both fractions were able to form biofilms, although the

initial biomass accumulation of both was slower than in the control third-generation biofilm (Figure 3.4B, D). Here, it is possible that the cells were stressed during cell sorting, leading to slower biomass accumulation. Alternatively, the high speed of biomass accumulation found in the control third generation might be a product of both fractions coexisting, rather than purely a function of the yellow adaptation. This conclusion is consistent with our observation that the adapted yellow cells can stick, but do not colonize the substrate as effectively as blue cells (see also Appendix B.5).

The YFP+ fraction biofilm accumulated biomass more quickly and accrued more total biomass than the first-generation yellow population control (Figures 3.2A, 3.4D). We concluded from this that the yellow population did, indeed, undergo some form of adaptation. To test whether the enhanced ability of the yellow population to form biofilms was a reversible change, we passed a subset of cells from the YFP+ fraction through growth on solid and in liquid media before inoculating into fresh flow cells. The growth of this population mirrored the behavior of the first-generation yellow population control—it formed no biofilm within 72 hours—suggesting that a reversible adaptation (perhaps a genetic polymorphism, or a regulatory change, or both) was responsible for the improved ability of the yellow population to form biofilms. Because the biofilm formed by the YFP+ fraction initially accumulated biomass more slowly, and accumulated less maximum total biomass, than the aggregate fraction biofilm, the adaptation of the yellow population alone cannot confer the growth advantage that we observed in the untreated second-generation biofilm (Figure 3.4A, D). Furthermore, we observed flat structure in the YFP+ fraction biofilm, indicating that it was unable to form healthy three-dimensional structure.

The biofilm formed by the aggregate fraction accumulated biomass more quickly, and also accumulated more total biomass, than the YFP+ fraction biofilm (Figure 3.4D). Total biomass accumulation of the aggregate fraction biofilm was twice that of the YFP+ fraction biofilm (Figure 3.4D). Together, all of these results suggest that the presence of aggregates is necessary for the speed of biomass accumulation and is sufficient to optimize total biomass accumulation. Additionally, the aggregated fraction biofilm starts with the emergent structure—the yellow population resides above the blue population from the start of the lifespan of the biofilm—which appears to enable both the blue and the yellow populations to recover and grow away from the substrate together (Figure 3.4D). Noting that the emergent structure did not re-emerge in the control third-generation biofilm, this indicates that inoculating only the aggregates recovers structure that is otherwise lost in the presence of the full effluent from the treated biofilm. These results demonstrate that the aggregates are at least correlated with the presence of the emergent structure.

### **3.11 Discussion and conclusion**

We constructed a synthetic symbiotic consortium from two populations of engineered *E. coli* that functions stably over long periods of time and through multiple population bottlenecks. After the consortium grew for 80 hours, we observed emergent structure which could be transferred to downstream environments and was correlated with a growth advantage (more total and faster biomass accumulation). Only when aggregates of the two populations were preserved through population bottlenecks were the emergent structure and greater total accumulation of biomass found in downstream biofilms. The

secondary component of the growth advantage, faster biomass accumulation, is the combined effect of an adaptive change in the yellow population, which enabled cells of the yellow population to adhere better, and the presence of aggregates of both populations.

Overall, these results suggest that aggregates are the primary conveyors of the emergent structure and the growth advantage of the consortium; the adaptive change in the yellow population, which hastens biofilm formation, also threatens to take over and dismantle the consortium if the aggregates are disrupted during population bottlenecks. If the yellow population takes over, the resulting uniform population is less well adapted than the consortium, as measured by the speed and amount of biomass accumulation.

The aggregates may preserve emergent structure by being readily assembled pieces of that structure, but how they convey a growth advantage is an open question. Aggregates may colonize a fresh substrate in a manner that enables more biomass to accumulate, or they may provide proximity between the two populations to enhance cooperation and growth. Either way, we see that three-dimensional structure is indeed an important mechanism that promotes optimal downstream colonization by the whole community, via aggregate detachment and downstream re-attachment. The spatial organization of the community into aggregates provides for both populations to survive, and to be inherited together so that the community functions better in a new environment (as measured by speed and amount of biomass accumulation) than either population can alone. As best we can tell, the aggregates are composed of 1/3 blue and 2/3 yellow biomass. It would be interesting to explore whether there is an optimal composition by artificially constructing and inoculating aggregates of varying composition.

In nature, it is likely that mixed populations attain spatial structure together that is conducive to their collaboration. The stable spatial structure afforded by biofilms provides for prolonged interactions between neighbors and for the development of emergent structure in communities [105, 106]. Selection then acts not just upon individual populations, but upon whole communities, and structures that enable communities to colonize downstream environments better than their constituent populations may be conserved through evolution. This engineered symbiotic consortium allowed us to uncover and study such interactions precisely, demonstrating the utility of engineered synthetic consortia to a wide range of scientific fields.

## 3.12 Methods

### 3.12.1 Strains and plasmids

Strains MGd- and MGfwc- were constructed by recombination with the lambda red recombinase plasmid pKD46, as outlined in [150]. More information about strain construction can be found in Appendix B.1. Plasmids were constructed as outlined in the text and in [42].

### 3.12.2 Growth conditions

Throughout all experiments, cultures and biofilms were grown at 30°C in M9-AADO medium containing 50  $\mu\text{gml}^{-1}$  kanamycin and 20  $\mu\text{gml}^{-1}$  tetracycline to maintain the engineered and the marker plasmids, respectively [68].

**M9-AADO** (*per litre*): 200 mL 5xM9, 100 mL 10x Amino Acid Dropout Solution without Lysine, 2 mM  $\text{MgSO}_4$ , 0.5% glycerol, 0.01% thymine.

**5x M9** (*per litre*): 18g anhydrous  $\text{Na}_2\text{HPO}_4$ , 15g  $\text{KH}_2\text{PO}_4$ , 5g  $\text{NH}_4\text{Cl}$ , 2.5g  $\text{NaCl}$ .

**10x Amino Acid Dropout Solution without Lysine** (*per litre*): 300 mg L-Isoleucine; 1500 mg L-Valine; 200 mg L-Adenine hemisulfate salt; 200 mg L-Arginine HCl; 200 mg L-Histidine HCl monohydrate; 1000mg L-Leucine; 200 mg L-Methionine; 500mg L-Phenylalanine; 2000 mg L-Threonine; 200 mg L-Tryptophan; 300 mg L-Tyrosine; 200 mg L-Uracil.

### 3.12.3 Biofilm preparation and inoculation

The biofilm flow apparatus was described previously in Chapter 2 and Appendix A.4 [42] with two exceptions. First, here inoculation was performed into the Tygon tubing via inoculation ports installed into three-way connectors one inch upstream of each flow lane (connectors, Cole Parmer and inoculation ports). Second, two inches of tubing upstream of flow lanes, including the inoculation port, was removed within 48 hours of inoculation to prevent upstream biofilm formation from affecting results within the flow cells. To begin first-generation biofilms, separate overnight cultures of blue and yellow populations were shaken in M9-AADO medium with antibiotics, as described above, to saturation. Cultures of the blue population were supplemented with 10  $\mu\text{M}$  C4HSL (Sigma, O9945). Cultures were centrifuged at 4000 RPM for 8 minutes, cells were re-suspended in 1mL 0.9% NaCl solution containing the same antibiotics, then diluted into 0.9% NaCl solution with the antibiotics to an  $\text{OD}_{600}$  of 0.07, which corresponds to approximately  $4 \times 10^7$  cells  $\text{mL}^{-1}$ . 1 mL of a 50/50 mixture of blue and yellow cells was inoculated into each flow lane for experimental replicates. Control lanes contained a 50/50 mixture of blue or yellow cells and 0.9% NaCl solution.

To begin untreated second- and third-generation biofilms, effluents from three separate replicates (in separate lanes) of the generation to be propagated were mixed,  $\text{OD}_{600}$  was adjusted to 0.07 as necessary, and 1 mL was inoculated into each fresh flow lane. To begin treated second-generation biofilms, effluents were taken as above, but prior to adjusting the  $\text{OD}_{600}$  the effluent was vortexed at top speed for 5 minutes and then

passed through a 40  $\mu\text{m}$  cell strainer (BD Falcon, #352340). All inoculates were plated in parallel with inoculation to confirm cell counts.

Prior to inoculation each 1x4x40 mm lane of each flow chamber (Stovall Life Sciences, ACFL0001) was incubated for at least 90 minutes at 37°C with 200  $\mu\text{L}$  of a solution of 10 mg/mL bovine ribonuclease B (Sigma, R7884) suspended in 0.02 M bicarbonate buffer. Each lane was then quenched with 200  $\mu\text{L}$  of 0.2% Bovine Serum Albumin (Sigma, A4503). Flow of M9-AADO with antibiotics through the flow chambers was initiated for five minutes prior to inoculation. After inoculation, flow chambers were incubated glass-coverslip-down for 4 minutes, and then flow was reinstated for 4 minutes prior to returning the flow chambers to the upright position. The flow rate of medium through each lane was approximately 230  $\mu\text{Lmin}^{-1}$  and flow cells were incubated at 30°C  $\pm$  2°C throughout the length of each experiment. Medium reservoirs were replaced every 12 hours to ensure freshness of the antibiotics.

#### **3.12.4 Imaging**

Images of the biofilms were captured with a Zeiss 510 upright confocal laser scanning microscope (CLSM), controlled by Carl Zeiss AIM. A Zeiss Achroplan 40x/0.8 W objective was used to capture all images, images were captured with 512x512 pixel resolution, and all image stacks were captured with identical pinhole and gain settings. eCFP excitation: 458 nm Argon laser, emission filter: BP 480–520 nm. eYFP excitation: 514 nm Argon laser, emission filter: LP 530 nm.

### **3.12.5 Metrics**

Measurements were calculated using the COMSTAT biofilm image processing package in Matlab. At least three biological replicates were grown at a time for each condition, and every condition was repeated on at least two different days. Averages were taken of COMSTAT results from at least three randomly selected images, taken at a variety of locations within the flow lane. More information about quantitative processing in COMSTAT, and changes made to COMSTAT to incorporate calculations of the biomass median can be found in Appendix B.3.